Check for updates

American Journal of Biological Anthropology

WILEY

AMERICAN JOURNAL OF BIOLOGICAL ANTHROPOLOGY

BRIEF COMMUNICATION OPEN ACCESS

Rib Cross-Sectional Mineralized Area in Early Pleistocene Hominins: Insights From the *Homo antecessor* and *H. erectus* s. l. Fossil Record

J. M. López-Rey[1,2] | D. García-Martínez[2,3,4] | A. Gómez-Olivencia[5,6,7] | O. Cambra-Moo[2] | A. González-Martín[2] | M. Bastir[1] | J. M. Bermúdez de Castro[8]

[1]Paleoanthropology Group, Department of Paleobiology, Museo Nacional de Ciencias Naturales (MNCN-CSIC), Madrid, Spain | [2]Department of Biology, Faculty of Sciences, Laboratorio de Poblaciones del Pasado (LAPP), Universidad Autónoma de Madrid (UAM), Madrid, Spain | [3]Physical Anthropology Unit, Faculty of Biological Sciences, Universidad Complutense de Madrid (UCM), Madrid, Spain | [4]Department of Life Sciences, Center for Functional Ecology - Science for People and the Planet (CFE), Laboratory of Forensic Anthropology, Centre for Functional Ecology, University of Coimbra (UC), Coimbra, Portugal | [5]Departamento de Geología, Facultad de Ciencia y Tecnología, Universidad del País Vasco-Euskal Herriko Unibertsitatea (UPV/EHU), Leioa, Spain | [6]Sociedad de Ciencias Aranzadi, Donostia-San Sebastián, Spain | [7]Centro Mixto (UCM-ISCIII) de Evolución y Comportamiento Humano, Madrid, Spain | [8]Centro Nacional de Investigación sobre la Evolución Humana (CENIEH), Burgos, Spain

Correspondence: J. M. López-Rey (jolopezr@mncn.csic.es)

Received: 11 July 2025 | **Revised:** 4 June 2026 | **Accepted:** 11 June 2026

Keywords: costal series | Gran Dolina | hominins | Nariokotome Boy | ontogeny

ABSTRACT

Objectives: Rib cross-sectional mineralized area provides valuable insights into mechanical loading and bone growth and remodeling. Given the scarcity of Early Pleistocene costal remains in the context of human evolution, we aimed to study the cross-sectional anatomy of fossil ribs from that period and compare them to a modern human ontogenetic series ranging from 8 to over 30 years of age.

Materials and Methods: We extracted the rib cross section at the midshaft of 6 fossil ribs attributed to several H. antecessor individuals and 10 fossil ribs of the *H. erectus* s. l. specimen KNM-WT 15000. Then we compared their relative mineralized area with that of the full, unilateral costal series of 27 *H. sapiens* individuals spanning different ontogenetic stages (pre-pubescent, post-pubescent, adult).

Results: Our findings indicate that rib cross-sectional mineralized area of H. antecessor is close to that of subadult *H. sapiens*, sharing a similar U-shaped trend along the costal series. Values are considerably lower compared to KNM-WT 15000, which shows a higher mineralized area at the middle thoracic rib levels rather than at the extremes.

Discussion: Despite possible taphonomic alteration of fossil ribs, these results suggest a different, possibly derived pattern of rib cross-sectional mineralized area in H. antecessor compared to more primitive Early Pleistocene hominins. However, considering the earlier ontogenetic stage of KNM-WT 15000, we cannot discard that ribs of H. antecessor belong to individuals exhibiting a postcranial growth pattern similar to that of *H. erectus* s. l., but at a more advanced phase in development.

1 | Introduction

The study of hominin ribs provides interesting data regarding the evolution of body shape, breathing kinematics, posture, and even locomotion, while also serving as important indicators of systemic health, nutritional status, and disease (e.g., Haile-Selassie et al. 2010; Schmid et al. 2013; García-Martínez et al. 2018; Gómez-Olivencia et al. 2018; Buikstra 2019; Bastir et al. 2022). However, publications on the topic have been limited due to several reasons. First, the fragility of these bones

This is an open access article under the terms of the Creative Commons Attribution-NonCommercial License, which permits use, distribution and reproduction in any medium, provided the original work is properly cited and is not used for commercial purposes.

© 2026 The Author(s). *American Journal of Biological Anthropology* published by Wiley Periodicals LLC.

often results in their absence from the fossil record. If present at archaeological sites, ribs are frequently fragmented, disarticulated, and commingled (Manifold 2012; Schotsmans et al. 2017; Abdel-Maksoud et al. 2022). In addition, the difficulty to amass reasonable comparative samples make ribs to be less studied than other anatomical regions in the "classical" monographs devoted to fossil hominins (e.g., Heim 1976; Vandermeersch 1981; Trinkaus 1983).

The development of new technologies during recent years has enabled a more in-depth study of the hominin thorax, leading to several high-resolution 3D ribcage reconstructions of fossil specimens such as KNM-WT 15000 (Nariokotome Boy, *H. erectus* s. l., ~1.53 Ma; Bastir et al. 2020), Kebara 2, Shanidar 3 (*H. neanderthalensis*, ~0.06 Ma; Gómez-Olivencia et al. 2018; López-Rey, García-Martínez, and Bastir 2025), or Dolní Věstonice 13 (*H. sapiens*, ~0.03 Ma; López-Rey, Crevecoeur, et al. 2025). These reconstructions also include some Neanderthal immature individuals at different ages-at-death, whose ribcage analysis has provided interesting data on growth trajectories in fossil hominins compared to modern humans (García-Martínez et al. 2020).

While costovertebral remains are relatively abundant for taxa such as *Australopithecus* (e.g., Clarke 2019; Schmid 1983; Schmid et al. 2013), Neanderthals (e.g., Franciscus and Churchill 2002; Gómez-Olivencia et al. 2009, 2019; García-Martínez et al. 2020; Bastir et al. 2022), and *H. sapiens* (e.g., López-Rey, Crevecoeur, et al. 2025), there is a particular scarcity of ribs in the hominin fossil record around the one-million-year mark. Consequently, there is a major gap in our understanding of thoracic evolution from specimens attributed to *H. erectus* s. l. to those dating near the divergence of the Neanderthal and *H. sapiens* lineages, a period in which the *H. antecessor* ribs are placed (~0.9 Ma; Carbonell et al. 1995; Bermúdez de Castro et al. 1997, 2017).

Among the postcranial elements recovered from the Gran Dolina-TD6 level (Sierra de Atapuerca, Burgos, Spain), six exceptionally preserved ribs assigned to *H. antecessor* stand out as particularly valuable for bridging this anatomical and chronological gap (Carretero et al. 1999; Gómez-Olivencia et al. 2010). Together with the costal remains of the Nariokotome Boy—so far the only well-preserved ribcage of *H. erectus* s. l. (Jellema et al. 1993; Haeusler et al. 2011)—, these bones offer a unique opportunity to investigate aspects of thoracic morphology, respiratory mechanics, and even Bauplan in Early Pleistocene hominins. Furthermore, remains belonging to these fossil individuals are interesting in terms of growth and development since none of them has reached full maturity according to modern human standards (Cunningham et al. 2016).

Regarding *H. antecessor*, Gómez-Olivencia et al. (2010) suggested that the aforementioned ribs belonged to pubescent and/or young adult individuals according to the fusion of three secondary centers of ossification: the head, articular, and nonarticular tubercles (Ríos and Cardoso 2009). Since they were missing in ribs like ATD6-85 and ATD6-97, the age-at-death of these individuals was tentatively estimated based on surface porosity and muscular scar rugosity in comparison with other ribs of the sample (Gómez-Olivencia et al. 2010). The case of the Nariokotome Boy presents a more nuanced scenario since his dental and skeletal ages are discordant. Dentally, KNM-WT 15000 presents eruption patterns suggesting an age of around 8–9 years. In contrast, his postcranial development aligns more closely with that of an individual aged 11–13 years, based on (1) the initiation of elbow joint ossification and (2) the absence of fusion in the remaining major long bone epiphyses (Dean and Smith 2009). This discrepancy has sparked considerable debate and underscores the challenges of assessing growth and maturation in extinct hominins, whose developmental patterns may have differed significantly from those of modern humans (Smith 2004).

In this context, García-Martínez et al. (2017) and López-Rey et al. (2022) revisited the classic hypothesis proposed by Schmid (1983), which suggests that variables of the rib cross section can predict overall rib (even thorax) configuration, which is especially relevant for the study of the often highly fragmented costal remains in the hominin fossil record. Particularly, López-Rey et al. (2022) and López-Rey, Doe, et al. (2025) propose that the percentage of mineralized area (% Min. Ar.) of the rib cross sections at the midshaft can serve as a proxy for mechanical loading and the biological processes shaping bone growth and remodeling. Given the immaturity of the most complete *H. erectus* s. l. and *H. antecessor* costal remains (Dean and Smith 2009; Gómez-Olivencia et al. 2010), a key question arises: do their cross-sectional mineralized areas (%) and the trends observed along their costal series resemble those of *H. sapiens* at comparable ontogenetic stages?

There is no straightforward answer, as addressing this issue requires a comprehensive comparative framework integrating morphological, biomechanical, and developmental perspectives. Furthermore, the study of cross-sectional variables in fossil specimens requires careful consideration of potential taphonomic and diagenetic alterations that may affect the internal structure of bone, particularly within the medullary space (e.g., Collins et al. 2002; Turner–Walker and Syversen 2002; Manifold 2012; Schotsmans et al. 2017). Such processes may increase the apparent proportion of mineralized area in fossil ribs, potentially biasing quantitative estimates derived from (micro-)CT data.

Considering these limitations, the aim of the present article is to make an exploratory study of the rib cross sections at the midshaft belonging to immature fossil hominins classified as *H. erectus* s. l. and *H. antecessor*. Their rib cross sections will be compared to those of medieval *H. sapiens* at different ontogenetic stages in order to unveil potential similarities or differences among species, and to assess how these may reflect broader evolutionary shifts in development within the genus *Homo*.

2 | Materials and Methods

For this research, we selected the six already published fossil ribs belonging to a minimum of three individuals of the TD6 hominins (*H. antecessor*, 0.85 ± 0.1 Ma BP, housed at the *Centro Nacional de Investigación sobre la Evolución Humana* [*CENIEH*], Burgos, Spain; Carretero et al. 1999; Gómez-Olivencia et al. 2010), and ten ribs belonging to specimen

26927691, 2026, 2, Downloaded from https://onlinelibrary.wiley.com/doi/10.1002/ajpa.70299 by Universidad De Burgos, Wiley Online Library on [31/07/2026]. See the Terms and Conditions (https://onlinelibrary.wiley.com/terms-and-conditions) on Wiley Online Library for rules of use; OA articles are governed by the applicable Creative Commons License

KNM-WT 15000 (Nariokotome Boy, *H. erectus* s. l., ~1.53 Ma BP, housed at the *Kenya National Museum* [*KNM*], Nairobi; Jellema et al. 1993). Our selection criteria required that the rib corpus was sufficiently preserved to allow the extraction of a cross section at the midshaft. While ribs from the TD6 hominins were micro-CT scanned at the *CENIEH* facilities, using a V|Tome|X s 240 equipment (GE Sensing & Inspections Technologies) with the following specifications: resolution = 90 μm; kV = 110; uA = 100; the original ribs and vertebrae of KNM-WT 15000 were scanned at the *Muthithi Medical Centre* (*Aga Khan University Hospital*, Nairobi, Kenya) by computed tomography (CT) with a SOMATOM Sensation 16 clinical scanner (Siemens) with these parameters: slice thickness = 0.75 mm; voxel size = $0.21 \times 0.21 \times 0.30\ mm^3$ (Bastir et al. 2020). *H. antecessor* ribs were sorted following Gómez-Olivencia et al. (2010), and ribs of the Nariokotome Boy were sorted according to Haeusler et al. (2011).

All fossil ribs were compared to a sample of *H. sapiens* from medieval Christian cemeteries located in the northwestern Iberian Peninsula. These costal remains were free from pathological or taphonomical damage that could distort rib anatomy. Given the immaturity described for some of the fossil material, comparative *H. sapiens* individuals were selected to match equivalent stages of skeletal development. These individuals were grouped into three categories: pre-pubescents (8–11 years old), post-pubescents (17–25 years old, incomplete fusion of their epiphyses), and a control group of adults (> 30 years old, all epiphyses fused). Specifically, the study included seven pre-pubescent and seven post-pubescent individuals from the Veranes cemetery (Gijón, Asturias, Spain; Rascón Pérez et al. 2013), as well as three post-pubescent and ten adults from the Marialba de la Ribera cemetery (Villaturiel, León, Spain; Candelas González et al. 2016).

Such as done by Doe et al. (2025), puberty status was determined using standard methods (Shapland and Lewis 2013, 2014; Lewis et al. 2016), while age-at-death was estimated through the examination of permanent mandibular dentition (Moorrees et al. 1963; Liversidge and Marsden 2010) and skeletal maturation (Lewis et al. 2016) when dental development was complete. It should be noted that estimating chronological age in adult skeletal remains beyond early adulthood remains inherently imprecise. In our study, individuals categorized as "> 30 years old" were assigned to this broad age class because currently available osteological indicators lose reliability once developmental and young adult features have fully matured. Further subdivision of adult individuals (e.g., into ranges such as 30–40 or 40–50 years) would therefore introduce a high risk of speculative age attribution rather than improving accuracy.

Regarding sex determination, pre-pubescent individuals were recorded as indeterminate due to the difficulties and potential inaccuracies associated with sexing at this ontogenetic stage. For the remaining individuals in the control sample, sex was assessed based on pelvic (Phenice 1969) and humeral features (Bass 2005) using the DSP method (Discriminant Function for Sex Prediction; Murail et al. 2005; Brůžek et al. 2017). This statistical approach employs specific osteometric measurements to calculate a discriminant function, providing a probabilistic estimation of an individual's sex.

Table 1 provides more information about the chosen sample, which was curated in the osteoarcheological collections housed at the *Laboratorio de Poblaciones del Pasado* (*LAPP*, Department of Biology, Faculty of Sciences, *Universidad Autónoma de Madrid*, Spain). For each individual, the best-preserved rib of each costal level was scanned via micro-CT at the *CENIEH* facilities, using a V|Tome|X s 240 equipment (GE Sensing & Inspections Technologies) with the following specifications: resolution = 90 μm; kV = 110; μA = 100. Since only one rib per costal level was analyzed, potential effects of bilateral thoracic asymmetry, which could affect bone cross-sectional properties (e.g., Wilson and Humphrey 2015), were not addressed.

The final rib volumes were reconstructed and saved in DICOM format to extract their cross sections at the midshaft using Slicer v. 5.6.2 (Fedorov et al. 2012) following the protocol previously published by López-Rey et al. (2022). First, we drew a straight line from the lateral (sternal) margin of the costal tubercle to the most ventral point of the sternal end of the rib (tuberculo-ventral chord; Franciscus and Churchill 2002). Next, we determined its bisection and extracted the cross section at the point where that bisection crossed the rib corpus, which we considered as the midshaft. This approach represents an approximation, as the ribs, although exceptionally preserved, were not entirely complete in some cases. Images containing these cross sections were subsequently saved in TIFF format.

We adopted the approach proposed by Andronowski and Crowder (2019) and studied the entire rib cross sections, as distinguishing cortical from trabecular bone can be subjective, particularly due to age-related trabecularization of the endosteal region. By including both cortical and trabecular bone in a single measure, observer-dependent variability is minimized, improving the repeatability and robustness of the measurement. Importantly, this approach captures the full mineralized fraction of the rib cross section, which is directly relevant for our study of ontogenetic patterns and evolutionary comparisons.

Once we extracted all the rib cross sections, we calculated relative bone area (Andronowski and Crowder 2019) as the percentage of mineralized area (% Min. Ar.) using Fiji-Image J v. 2.1.0/1.53s (Schindelin et al. 2012). For that purpose, this software provides a threshold that allows differentiation between mineralized area (including both cortical and trabecular components, regardless of whether it has undergone diagenetic replacement of the original organic matrix) and non-mineralized spaces (which in life would have been occupied by marrow and vascular structures). In our case, we provided a brightness threshold of 50 (out of 255) to RGB color images in the module *Adjust* ➔ *Color threshold*. Knowing the total area of each cross section, we determined the % Min. Ar. of the sample (Table 2, Supplementary Table S1) and then studied its graphical distribution using line plots with error bars (Figure 1). Unfortunately, the extracted cross section of fossil rib ATD6-108 (costal level 1) was fragmented. Taking into consideration that its preserved epiphysis (articular tubercle) is fused (Gómez-Olivencia et al. 2010), we decided to complete its missing part using the first rib cross sections of individuals ID 87 and 120.1 of our comparative sample as they respectively had the highest and lowest % Min. Ar. among all adult *H. sapiens* first ribs. From the selected rib cross section of ATD6-108 we subsequently obtained two estimations (ATD6-108a and ATD6-108b), depicted in Figure 1.

26927691, 2026, 2, Downloaded from https://onlinelibrary.wiley.com/doi/10.1002/ajpa.70299 by Universidad De Burgos, Wiley Online Library on [31/07/2026]. See the Terms and Conditions (https://onlinelibrary.wiley.com/terms-and-conditions) on Wiley Online Library for rules of use; OA articles are governed by the applicable Creative Commons License

TABLE 1 | Expanded information about the comparative *H. sapiens* sample.

ID	Collection (UAM)	Sex	Age	Stage
47.1	Veranes (Asturias, Spain)	Indeterminate	10	Pre-pubescent
164			10	
310			9	
328			11	
451			10	
481			10	
539			8	
176	Marialba de la Ribera (León, Spain)	Male	15–20	Post-pubescent
195		Male	15–20	
197		Female	15–20	
137	Veranes (Asturias, Spain)	Male	20–25	Post-pubescent
249		Female	17	
295		Male	20–25	
320		Male	20–25	
489		Female	20–21	
586		Female	18	
601		Female	19	
70.1	Marialba de la Ribera (León, Spain)	Male	≥30	Adult
87		Female		
102		Female		
120.1		Male		
143		Male		
149		Female		
150		Female		
153		Female		
178		Male		
221		Female		

Although we had a consistent comparative sample of $n \geq 7$ ribs per group and costal level, fossil ribs are unique, which required the use of a sufficiently robust statistical approach to interpret the results correctly. Therefore, we implemented a nonparametric bootstrap test to ensure reliable inferences from the available data (Dwivedi et al. 2017). This approach consists of calculating 95% confidence intervals (CIs) of the mean by resampling 1000 times the data of the control sample per costal level. Then the test checks whether fossil values fall within these CIs. For fossil ribs that could potentially be assigned to different costal levels (e.g., ATD6-85), comparisons were made with all corresponding ribs from the control sample. Statistical analyses were performed in RStudio v. 2023.12.1-402 (R Core Team 2023) using the packages "boot" v. 1.3–31 (Canty and Ripley 2024), "dplyr" v. 1.1.4 (Wickham et al. 2023), "ggplot2" v. 3.3.3 (Wickham 2016), and "tidyr" v. 1.3.1 (Wickham et al. 2024). The full R script is included in the Supporting Information.

3 | Results

Rib cross sections of adult *H. sapiens* have a lower percentage of mineralized area (% Min. Ar.) compared to pre- and post-pubescents. While all *H. antecessor* rib cross sections fall within the current human range of variation (most of them exclusively within the subadult range), more than half of the studied *H. erectus* s. l. rib cross sections have a higher % Min. Ar. than that of any *H. sapiens* (Figure 1, Table 2). Moreover, most % Min. Ar. of both *H. antecessor* and *H. erectus* s. l. exceed the 95% confidence intervals of the mean % Min. Ar. calculated for *H. sapiens* (Table 3). The graphical distribution of the data is similar between *H. antecessor* and *H. sapiens*, with maximum values at the extreme costal levels and minimum values at the central ones (Figure 1). This trend is maintained when the % Min. Ar. of rib ATD6-108 is considered between the two estimations (ATD6-108a and ATD6-108b). Curiously,

26927691, 2026, 2, Downloaded from https://onlinelibrary.wiley.com/doi/10.1002/ajpa.70299 by Universidad De Burgos, Wiley Online Library on [31/07/2026]. See the Terms and Conditions (https://onlinelibrary.wiley.com/terms-and-conditions) on Wiley Online Library for rules of use; OA articles are governed by the applicable Creative Commons License

TABLE 2 | Rib cross-sectional mineralized area (%) of the sample. Data from the comparative *H. sapiens* sample has been summarized using the mean ± standard deviation.

H. antecessor **(TD6)**			***H. erectus*** **s.l. (KNM-WT 15000)**			**H. sapiens**					
Post-pubescent or adult			**Pre-pubescent**			**Pre-pubescent**		**Post-pubescent**		**Adult**	
ID	**Costal level[a]**	**% Min. Ar[b]**	**ID**	**Costal level[c]**	**% Min. Ar[b]**	**Costal level**	**% Min. Ar[b]**	**Costal level**	**% Min. Ar[b]**	**Costal level**	**% Min. Ar[b]**
ATD6-108a	1 (R)[d]	88.43	AY&AZ	1 (R)	96.60	1	82.78 ± 7.60	1	84.80 ± 5.77	1	76.64 ± 6.18
ATD6-108b	1 (R)	81.92	AQ	2 (L)	84.06	2	73.28 ± 4.90	2	74.05 ± 10.67	2	63.93 ± 8.91
ATD6-79	2 (R)	69.6	AT	3 (L)	74.78	3	71.42 ± 7.04	3	71.87 ± 9.12	3	60.93 ± 11.57
ATD6-89 + 206	7 (L)[e]	80.73	CB	5 (L)	96.00	4	67.63 ± 4.70	4	69.68 ± 10.14	4	59.75 ± 8.30
ATD6-85	8–10 (R)	82.17	AL	6 (R)	92.00	5	68.29 ± 7.05	5	69.76 ± 10.11	5	58.68 ± 6.34
ATD6-39	10 (L)	85.38	BR	8 (L)	84.68	6	69.16 ± 7.70	6	72.54 ± 7.07	6	61.93 ± 6.12
ATD6-97	10–11 (L)	86.34	AU	9 (L)	85.10	7	71.81 ± 5.50	7	74.68 ± 8.07	7	63.10 ± 7.67
			AO	10 (L)	94.51	8	70.67 ± 5.80	8	74.69 ± 5.60	8	64.38 ± 11.67
			AJ	11 (R)	85.89	9	75.85 ± 7.50	9	74.85 ± 5.18	9	67.06 ± 8.78
			AN	12(L)	76.08	10	80.55 ± 6.04	10	79.63 ± 6.48	10	71.03 ± 7.05
						11	83.24 ± 7.02	11	82.51 ± 6.04	11	73.97 ± 4.61
						12	85.79 ± 9.30	12	87.07 ± 4.42	12	79.15 ± 7.10

[a]Ribs sorted according to Gómez-Olivencia et al. (2010).
[b]Percentage of mineralized area of the rib cross section at the midshaft.
[c]Ribs sorted according to Haeusler et al. (2011).
[d]Right side.
[e]Left side.

26927691, 2026, 2, Downloaded from https://onlinelibrary.wiley.com/doi/10.1002/ajpa.70299 by Universidad De Burgos, Wiley Online Library on [31/07/2026]. See the Terms and Conditions (https://onlinelibrary.wiley.com/terms-and-conditions) on Wiley Online Library for rules of use; OA articles are governed by the applicable Creative Commons License

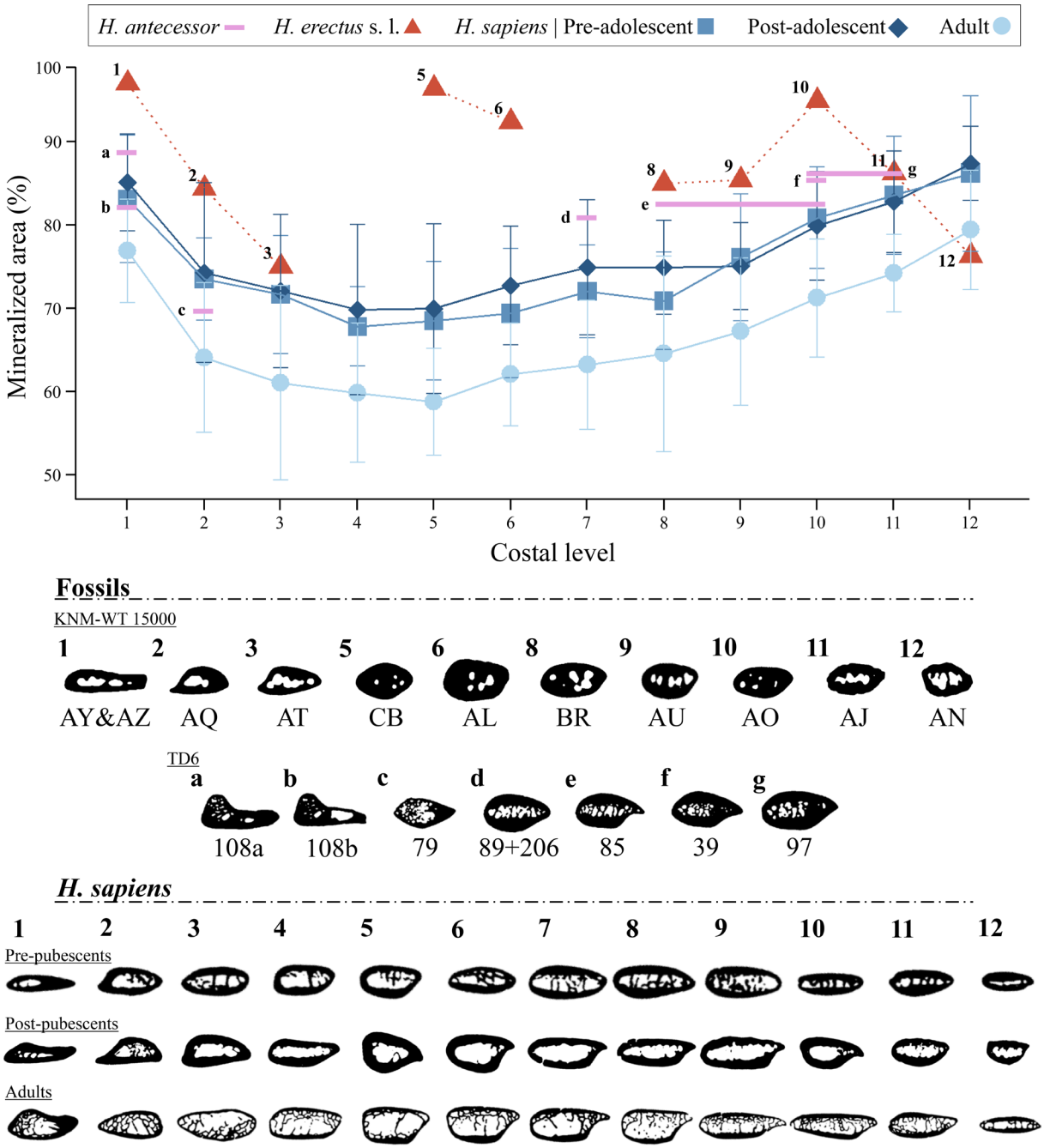

FIGURE 1 | Plot depicting the percentage of mineralized area (% Min. Ar.) of the studied rib cross sections, as well as the selected rib cross sections of KNM-WT 15000, TD6, and a random individual of each *H. sapiens* age group. The relative size relationship among the ribs of each individual is proportional, but the cross sections have been scaled to better illustrate differences in % Min. Ar. For ribs 1 and 2, the upper part of the image corresponds to the cranial direction, whereas for the remaining ribs it corresponds to the cutaneous surface.

the U-shaped trend found in *H. antecessor* and *H. sapiens* is not shared by specimen KNM-WT 15000. Although the pattern of % Min. Ar. on the upper thorax resembles that of the rest of the sample (levels 1–3), it is extremely high in central ribs (levels 5 and 6), and relatively low in rib cross sections from levels 11 and 12 (Figure 1).

4 | Discussion

The distribution of the data in the comparative *H. sapiens* sample is consistent with previous studies in current populations (e.g., Bonicelli et al. 2022; Holcombe and Derstine 2022) and shows that adult *H. sapiens* have a lower percentage of mineralized area (% Min. Ar.) in their rib cross sections compared to pre- and post-pubescents (Figure 1, Table 2). While we cannot exclude the possibility that some adult individuals reached advanced ages, which could theoretically influence their % Min. Ar., this scenario is likely uncommon in the rural, medieval populations represented in our sample (Candelas González et al. 2016; Rascón Pérez et al. 2013). Historical demographic data suggest that survival to very old age was relatively rare, with life expectancy after adulthood typically remaining well below modern values, even in nobles (Cummins 2017).

26927691, 2026, 2, Downloaded from https://onlinelibrary.wiley.com/doi/10.1002/ajpa.70299 by Universidad De Burgos, Wiley Online Library on [31/07/2026]. See the Terms and Conditions (https://onlinelibrary.wiley.com/terms-and-conditions) on Wiley Online Library for rules of use; OA articles are governed by the applicable Creative Commons License

TABLE 3 | Results of the nonparametric bootstrap test (1000 resampling iterations).

Costal level	Group	CI[a] (95%)	Within CI[a]?							
			KNM-WT 15000	ATD6-108a	ATD6-108b	ATD6-79	ATD6-89+206	ATD6-85	ATD6-39	ATD6-97
1	Pre-pubescent	77.31–88.31	No	No	Yes					
	Post-pubescent	81.49–88.21			Yes					
	Adult	73.22–80.44			No					
2	Pre-pubescent	70.27–76.61	No			No				
	Post-pubescent	67.38–79.84				Yes				
	Adult	58.63–69				No				
3	Pre-pubescent	66.76–76.37	Yes							
	Post-pubescent	66.60–77.17	Yes							
	Adult	54.21–67.58	No							
5	Pre-pubescent	63.25–73.03	No							
	Post-pubescent	63.93–75.57								
	Adult	54.96–62.42								
6	Pre-pubescent	64.04–74.36	No							
	Post-pubescent	68.07–76.40								
	Adult	58.55–65.54								
7	Pre-pubescent	67.93–75.43					No			
	Post-pubescent	69.93–79.31								
	Adult	58.34–67.30								
8	Pre-pubescent	66.80–74.57	No					No		
	Post-pubescent	71.38–78								
	Adult	57.33–71.06								
9	Pre-pubescent	71.03–81.17	No					No		
	Post-pubescent	71.88–77.94								
	Adult	62.16–72.45								

(Continues)

26927691, 2026, 2, Downloaded from https://onlinelibrary.wiley.com/doi/10.1002/ajpa.70299 by Universidad De Burgos, Wiley Online Library on [31/07/2026]. See the Terms and Conditions (https://onlinelibrary.wiley.com/terms-and-conditions) on Wiley Online Library for rules of use; OA articles are governed by the applicable Creative Commons License

TABLE 3 | (Continued)

Costal level	Group	CI[a] (95%)	Within CI[a]?							
			KNM-WT 15000	ATD6-108a	ATD6-108b	ATD6-79	ATD6-89+206	ATD6-85	ATD6-39	ATD6-97
10	Pre-pubescent	76.66–84.77	No					Yes	No	No
	Post-pubescent	75.8–83.24						Yes		
	Adult	66.82–75.11						No		
11	Pre-pubescent	77.65–87.82	Yes							Yes
	Post-pubescent	78.96–86.03	Yes							No
	Adult	71.23–76.58	No							No
12	Pre-pubescent	78.71–92.07	No							
	Post-pubescent	84.44–89.69	No							
	Adult	74.91–83.11	Yes							

[a]Confidence interval.

Consequently, although age-related osteopenia could reduce the % Min. Ar. in some cases (Bonicelli et al. 2022; Holcombe and Derstine 2022), the probability that a substantial portion of the sample consisted of senescent individuals is considered low.

Regarding *H. antecessor*, although most ribs are above the 95% confidence interval (CI) of the *H. sapiens* comparative sample mean (Table 3), their % Min. Ar. is encompassed within the *H. sapiens* range of variation, especially in subadults (Figure 1, Table 2). This pattern contrasts with that of *H. erectus* s. l., whose cross-sectional % Min. Ar. is distinctly higher than those observed in *H. sapiens* (Figure 1, Table 2, Table 3). Such results are not surprising given the generally higher relative bone cross-sectional area proposed for fossil *Homo* (Chirchir et al. 2015; Ryan and Shaw 2015), the immaturity of the KNM-WT 15000 remains, and also the immaturity of, at least, part of the TD6 sample (Dean and Smith 2009; Gómez-Olivencia et al. 2010).

Additionally, these findings support the hypothesis of Schmid (1983) and García-Martínez et al. (2017), which proposed that cross-sectional variables would be linked to overall rib and even thorax morphology: rib cross sections with higher % Min. Ar. are linked to medio-laterally wider and antero-posteriorly deeper thoraces, such as the one described for the Nariokotome Boy (Bastir et al. 2020) and the one proposed for *H. antecessor* based on clavicular morphology and proportions (García-González et al. 2009).

Looking more closely at the distribution of data across costal levels (Figure 1), the three *H. sapiens* ontogenetic groups present a U-shaped trend, with maximum values at costal levels 1 and 12 and minimum values at costal levels 4–5. With the available data, the pattern observed in *H. antecessor* is similar to that of *H. sapiens*. It must be acknowledged, however, that a medial portion of the cross section of fossil rib ATD6-108 (costal level 1) was missing, and ATD6-108a and ATD6-108b are estimations. Although this represents a methodological limitation, the overall trend is maintained when considering the % Min. Ar. of rib ATD6-108 between these two reconstructions.

López-Rey et al. (2022) and López-Rey, Doe, et al. (2025) suggested that this U-shaped distribution might reflect mechanical stress associated with muscular attachments in these regions. In particular, the activity of the scalene muscles (ribs 1–2) and the diaphragm (ribs 7–12) during respiration might be associated with a higher % Min. Ar. in these rib cross sections (De Troyer and Boriek 2011; López-Rey et al. 2022, 2023). Although other muscles such as the levatores costarum, external intercostals, or serratus anterior also contribute to thoracic expansion during inspiration, these either span all costal levels or act across all the upper thorax (Gray 1878), making it difficult to attribute differential mineralization patterns to their action. In contrast, the scalenes and the diaphragm insert specifically at the rib levels showing higher % Min. Ar. in our dataset, making them the most biomechanically parsimonious explanation for the observed distribution.

Costal levels 4–5 have the lowest % Min. Ar. possibly because they are less actively involved in breathing kinematics (Graeber and Nazim 2007; De Troyer and Boriek 2011; López-Rey et al. 2022). Notably, the four costal levels whose cross sections have larger % Min. Ar. are those traditionally labeled "atypical" by the literature (levels 1, 2, 11, 12; Graeber and Nazim 2007). These ribs, which are significantly smaller and have a distinct shape compared to the rest of the ribcage, might require higher % Min. Ar. to maintain structural integrity under the stress produced by their muscle attachments.

26927691, 2026, 2, Downloaded from https://onlinelibrary.wiley.com/doi/10.1002/ajpa.70299 by Universidad De Burgos, Wiley Online Library on [31/07/2026]. See the Terms and Conditions (https://onlinelibrary.wiley.com/terms-and-conditions) on Wiley Online Library for rules of use; OA articles are governed by the applicable Creative Commons License

Curiously, the tendency observed in KNM-WT 15000 is different from that reported by the comparative *H. sapiens* sample since the % Min. Ar. calculated for the central costal levels is higher than that of the extremes. This pattern could be driven by several factors. The first is the different resolution of the scans, which may have affected the precision of the measurements due to an underestimation of bone porosity (García-Martínez et al. 2023). The potential effects of taphonomic distortion on these fossil rib cross sections must also be taken into consideration (Walker 1993). Beyond weathering, these ribs might have been exposed to diagenetic processes such as recrystallization, which can alter the density and appearance of bone in CT scans and potentially lead to overestimation of % Min. Ar. (Collins et al. 2002; Turner–Walker and Syversen 2002; Manifold 2012; Schotsmans et al. 2017). Although the impact of diagenetic alteration on the results may be beyond the scope of the present study to assess, it should be highlighted as an important caveat when interpreting the % Min. Ar. in fossil specimens.

If we assume that the aforementioned factors have not significantly affected our results, we might think that the observed pattern in KNM-WT 15000 could be a matter of ontogeny since human rib maturation occurs from the extreme to the central costal levels (Cunningham et al. 2016). Even so, the U-shaped trend in subadult *H. sapiens*—although less pronounced compared to adults—is evidently different from that of KNM-WT 15000. The only precedent to these results is the one found by López-Rey et al. (2022) for the rib cross sections of the immature *Australopithecus africanus* specimen Sts 14, whose tendency resembles the one found for KNM-WT 15000 in the present article. Future studies should further investigate rib maturation in *Australopithecus* and early *Homo* to determine what shared ontogenetic patterns or biomechanical constraints underlie similarities between these species.

Our results on the rib cross sections of *H. erectus* s. l. and *H. antecessor* open a new avenue of discussion within the already complex and controversial scenario surrounding hominin evolution during the Early Pleistocene. The present investigation shows that the hominin ribs recovered from the Gran Dolina-TD6 level have less cross-sectional % Min. Ar. than those of KNM-WT 15000, but what are the implications of these findings? On the one hand, it could be hypothesized that *H. antecessor* had different growth patterns compared to *H. erectus* s. l. This would not be unexpected since their fossil record is separated by more than half a million years. Moreover, these results would align with dental analyses conducted by Bermúdez de Castro et al. (1999, 2010), which suggest that developmental patterns in *H. antecessor* are more aligned to *H. sapiens* than to *H. erectus* s. l. Nonetheless, the only well-preserved rib series attributed to *H. erectus* s. l. comes from KNM-WT 15000, whose age at death has been estimated to correspond approximately to early pubescence (Dean and Smith 2009). In this context, the *H. antecessor ribs* studied here (estimated to belong to pubescent/young adult individuals (Gómez-Olivencia et al. 2010)) may represent more advanced ontogenetic stages with postcranial maturation patterns broadly aligned with that of *H. erectus* s. l.

However, such interpretations must be approached with caution since these exploratory results were obtained using a single, relative variable (% Min. Ar.), and it remains to be determined whether the observed patterns are also reflected in other cross-sectional properties, including absolute measurements (Andronowski and Crowder 2019). Beyond this, it has to be acknowledged that data from *H. antecessor* are inherently difficult to interpret. First, mid-thoracic ribs from *H. antecessor* individuals with an age-at-death comparable to that of the Nariokotome Boy should be found and studied to confirm the hypothesis presented in the previous paragraph. Second, the available costal remains of *H. antecessor* belong to different individuals with different ages-at-death, making it challenging to isolate a consistent developmental signal. Third, although it is proposed that *H. antecessor* had a more derived growth pattern than *H. erectus* s. l. (Bermúdez de Castro et al. 1999, 2010), the former might have exhibited faster maturation than *H. sapiens*, which complicates direct ontogenetic comparisons (Smith 2004).

In addition, it has to be taken into consideration that the *H. sapiens* comparative sample belongs to medieval populations from the Iberian Peninsula (Rascón Pérez et al. 2013; Candelas González et al. 2016). This entails certain inherent limitations. For instance, as noted in previous studies, adolescent growth in Iberian, medieval populations show significant variation depending on the site, likely due to differences in nutrition, health, and environmental conditions (e.g., Cardoso and Garcia 2009; Kors et al. 2025). This variability could lead to underestimation of age in the comparative sample, particularly for the most immature individuals. Furthermore, although these individuals likely engaged in regular physical activity due to their preindustrial lifestyle, they are not directly comparable to hunter-gatherer populations (Chirchir et al. 2015; Ryan and Shaw 2015). In the latter, daily biomechanical demands were presumably higher, which may have resulted in greater % Min. Ar. in their rib cross sections. Future research on Upper Paleolithic *H. sapiens* would be particularly interesting in this context, both for assessing intra-specific variability and for providing comparative samples with extinct hominins who exhibited more similar lifestyles.

5 | Conclusions

Homo antecessor and subadult *H. sapiens* share a similar percentage of mineralized area (% Min. Ar.) in their rib cross sections, as well as a similar U-shaped trend on these values along the costal series. Contrary, rib cross sections from *H. erectus* s. l. have a higher % Min. Ar. and the resulting data display a different trend. We hypothesize that both *H. erectus* s. l. and *H. antecessor* had different ontogenetic patterns regarding their rib cross sections. However, we cannot exclude the possibility that the ribs of *H. antecessor* belong to individuals exhibiting a postcranial growth pattern similar to that of *H. erectus* s. l., but at a later developmental stage. Importantly, potential diagenetic alterations could also interfere with the interpretation of % Min. Ar. in fossil specimens, and thus caution is warranted when drawing ontogenetic inferences.

Author Contributions

D. García-Martínez: conceptualization, investigation, funding acquisition, methodology, validation, writing – review and editing, software, formal analysis, project administration, supervision, resources, writing

26927691, 2026, 2, Downloaded from https://onlinelibrary.wiley.com/doi/10.1002/ajpa.70299 by Universidad De Burgos, Wiley Online Library on [31/07/2026]. See the Terms and Conditions (https://onlinelibrary.wiley.com/terms-and-conditions) on Wiley Online Library for rules of use; OA articles are governed by the applicable Creative Commons License

– original draft. **M. Bastir:** project administration, writing – review and editing, supervision, funding acquisition, validation, investigation. **O. Cambra-Moo:** investigation, validation, writing – review and editing, data curation, supervision, resources. **A. Gómez-Olivencia:** investigation, writing – review and editing, validation, supervision, writing – original draft. **A. González-Martín:** data curation, supervision, resources, validation, writing – review and editing, investigation. **J. M. López-Rey:** conceptualization, investigation, writing – original draft, methodology, writing – review and editing, visualization, software, formal analysis. **J. M. Bermúdez de Castro:** data curation, supervision, resources, writing – review and editing, validation, investigation.

Acknowledgments

We acknowledge Dr. Fred Spoor for the CT-scanning of KNM-WT 15000 thoracic material. In addition, we thank Dr. Nieves Candelas González and Dr. Danielle M. Doe for facilitating access to the sample recovered from the Marialba de la Ribera and Veranes cemeteries, respectively. Finally, we would like to highlight the importance of the work carried out by Belén Notario, who micro-CT scanned most of the sample at the *CENIEH* facilities.

Funding

JMLR is funded by the Spanish Ministry of Science and Innovation (Grant PRE2021-097584 linked to project PID2020-115854GB-I00 funded to M.B.). The Laboratorio de Poblaciones del Pasado (LAPP) is supported by projects PGC2018-099405-B-I00 (Spanish Ministry of Science, Innovation and Universities), HAR2016-78036-P (Spanish Ministry of Economy and Competitivity), and SI4/PJI/2024-00104 (Community of Madrid). This research is also supported by projects PID2021-122355NB-C33 and PID2024-156477NB-C33 (Spanish Ministry of Science and Innovation). A.G.O. is supported by Research Group IT1485-22 (Eusko Jaurlaritza-Gobierno Vasco), and by the Spanish Ministry of Science and Innovation (Project PID2021-122355NB-C31, MCIN/AEI/10.13039/501100011033/FEDER, UE).

Ethics Statement

We ensure adherence to ethical standards by respecting data provenance and the rights of individuals represented in the sample.

Conflicts of Interest

The authors declare no conflicts of interest.

Data Availability Statement

Original CT and micro-CT data of all individuals included in this study are available upon reasonable request from the respective host institutions: *Kenya National Museum* (*KNM*) for KNM-WT 15000, *Centro Nacional de Investigación sobre la Evolución Humana* (*CENIEH*) for TD6, and *Universidad Autónoma de Madrid* (*UAM*) for the *H. sapiens* comparative sample. Cross-sectional images derived from these datasets are subject to the same restrictions and must also be requested directly from the corresponding host institutions.

References

Abdel-Maksoud, G., H. E. S. Kira, and W. S. Mohamed. 2022. "Consolidation of Fragile Archaeological Bone Artifacts: A Review." *Egyptian Journal of Chemistry* 65: 1065–1080. https://doi.org/10.21608/EJCHEM.2022.158706.6860.

Andronowski, J. M., and C. Crowder. 2019. "Bone Area Histomorphometry." *Journal of Forensic Sciences* 64, no. 2: 486–493. https://doi.org/10.1111/1556-4029.13815.

Bass, W. M. 2005. *Human Osteology: A Laboratory and Field Manual*. Missouri Archaeological Society.

Bastir, M., D. García-Martínez, N. Torres-Tamayo, et al. 2020. "Rib Cage Anatomy in *Homo erectus* Suggests a Recent Evolutionary Origin of the Studied Upper Diaphragms." *Nature Ecology & Evolution* 4, no. 9: 1178–1187. https://doi.org/10.1038/s41559-020-1240-4.

Bastir, M., D. Sanz-Prieto, J. M. López-Rey, et al. 2022. "The Evolution, Form and Function of the Human Respiratory System." *Journal of Anthropological Sciences* 100: 141–172. https://doi.org/10.4436/jass.10014.

Bermúdez de Castro, J. M., J. L. Arsuaga, E. Carbonell, A. Rosas, I. Martínez, and M. Mosquera. 1997. "A Hominid From the Lower Pleistocene of Atapuerca, Spain: Possible Ancestor to Neandertals and Modern Humans." *Science* 276: 1392–1395. https://doi.org/10.1126/science.276.5317.1392.

Bermúdez de Castro, J. M., M. Martinón-Torres, J. L. Arsuaga, and E. Carbonell. 2017. "Twentieth Anniversary of *Homo antecessor* (1997-2017): A Review." *Evolutionary Anthropology* 26, no. 4: 157–171. https://doi.org/10.1002/evan.21540.

Bermúdez de Castro, J. M., M. Martinón-Torres, A. Gómez-Robles, et al. 2010. "New Immature Hominin Fossil From European Lower Pleistocene Shows the Earliest Evidence of a Modern Human Dental Development Pattern." *Proceedings of the National Academy of Sciences of the United States of America* 107: 11739–11744. https://doi.org/10.1073/pnas.1006772107.

Bermúdez de Castro, J. M., A. Rosas, E. Carbonell, M. E. Nicolás, J. Rodríguez, and J. L. Arsuaga. 1999. "A Modern Human Pattern of Dental Development in Lower Pleistocene Hominids From Atapuerca-TD6 (Spain)." *Proceedings of the National Academy of Sciences* 96: 4210–4213. https://doi.org/10.1073/pnas.96.7.4210.

Bonicelli, A., E. F. Kranioti, B. Xhemali, E. Arnold, and P. Zioupos. 2022. "Assessing Bone Maturity: Compositional and Mechanical Properties of Rib Cortical Bone at Different Ages." *Bone* 155: 116265. https://doi.org/10.1016/j.bone.2021.116265.

Brůžek, J., F. Santos, B. Dutailly, P. Murail, and E. Cunha. 2017. "Validation and Reliability of the Sex Estimation of the Human Os Coxae Using Freely Available DSP2 Software for Bioarchaeology and Forensic Anthropology." *American Journal of Physical Anthropology* 164, no. 2: 440–449. https://doi.org/10.1002/ajpa.23282.

Buikstra, J. E., ed. 2019. *Ortner's Identification of Pathological Conditions in Human Skeletal Remains*. Academic Press.

Candelas González, N., A. Núñez Cantalapiedra, H. Rascon Pérez, et al. 2016. "Características paleodemográficas de la poblacion recuperada del cementerio de Marialba de la Ribera (Villaturiel, Leon, España) (S. IV-XIII)." *Munibe Antropología-Arkeología* 67: 151–165. https://doi.org/10.21630/maa.2016.67.07.

Canty, A., and B. D. Ripley. 2024. "boot: Bootstrap R (S-Plus) Functions. . R package version 1.3-31." https://cran.r-project.org/web/packages/boot/index.html.

Carbonell, E., J. M. Bermúdez de Castro, J. L. Arsuaga, et al. 1995. "Lower Pleistocene Hominids and Artifacts From Atapuerca-TD6 (Spain)." *Science* 269: 826–830. https://doi.org/10.1126/science.7638598.

Cardoso, H. F., and S. Garcia. 2009. "The Not-So-Dark Ages: Ecology for Human Growth in Medieval and Early Twentieth Century Portugal as Inferred From Skeletal Growth Profiles." *American Journal of Physical Anthropology* 138, no. 2: 136–147. https://doi.org/10.1002/ajpa.20910.

Carretero, J. M., C. Lorenzo, and J. L. Arsuaga. 1999. "Axial and Appendicular Skeleton of *Homo antecessor*." *Journal of Human Evolution* 37, no. 3–4: 459–499. https://doi.org/10.1006/jhev.1999.0342.

Chirchir, H., T. L. Kivell, C. B. Ruff, et al. 2015. "Recent Origin of Low Trabecular Bone Density in Modern Humans." *Proceedings of the National Academy of Sciences* 112, no. 2: 366–371. https://doi.org/10.1073/pnas.1411696112.

26927691, 2026, 2, Downloaded from https://onlinelibrary.wiley.com/doi/10.1002/ajpa.70299 by Universidad De Burgos, Wiley Online Library on [31/07/2026]. See the Terms and Conditions (https://onlinelibrary.wiley.com/terms-and-conditions) on Wiley Online Library for rules of use; OA articles are governed by the applicable Creative Commons License

Clarke, R. J. 2019. "Excavation, Reconstruction and Taphonomy of the StW 573 *Australopithecus prometheus* Skeleton From Sterkfontein Caves, South Africa." *Journal of Human Evolution* 127: 41–53. https://doi.org/10.1016/j.jhevol.2018.11.010.

Collins, M. J., C. M. Nielsen–Marsh, J. Hiller, et al. 2002. "The Survival of Organic Matter in Bone: A Review." *Archaeometry* 44, no. 3: 383–394. https://doi.org/10.1111/1475-4754.t01-1-00071.

Cummins, N. 2017. "Lifespans of the European Elite, 800–1800." *Journal of Economic History* 77, no. 2: 406–439. https://doi.org/10.1017/S0022050717000468.

Cunningham, C., L. Scheuer, and S. Black. 2016. *Developmental juvenile osteology*. Academic press.

De Troyer, A., and A. M. Boriek. 2011. "Mechanics of the Respiratory Muscles." *Comprehensive Physiology* 1, no. 3: 1273–1300.

Dean, M. C., and B. H. Smith. 2009. "Growth and Development of the Nariokotome Youth, KNM-WT 15000." In *The First Humans – Origin and Early Evolution of the Genus Homo. Vertebrate Paleobiology and Paleoanthropology*, edited by F. E. Grine, J. G. Fleagle, and R. E. Leakey. Springer.

Doe, D. M., N. Candelas González, J. A. Gutiérrez González, O. Cambra-Moo, and A. González Martín. 2025. "Unlocking Adolescence: A Novel Approach to Approximate the Sociocultural Implications of Puberty in Medieval Spain." *American Journal of Human Biology* 37, no. 5: e70054. https://doi.org/10.1002/ajhb.70054.

Dwivedi, A. K., I. Mallawaarachchi, and L. A. Alvarado. 2017. "Analysis of Small Sample Size Studies Using Nonparametric Bootstrap Test With Pooled Resampling Method." *Statistics in Medicine* 36, no. 14: 2187–2205. https://doi.org/10.1002/sim.7263.

Fedorov, A., R. Beichel, J. Kalpathy-Cramer, et al. 2012. "3D Slicer as an Image Computing Platform for the Quantitative Imaging Network." *Magnetic Resonance Imaging* 30, no. 9: 1323–1341.

Franciscus, R. G., and S. E. Churchill. 2002. "The Costal Skeleton of Shanidar 3 and a Reappraisal of Neandertal Thoracic Morphology." *Journal of Human Evolution* 42, no. 3: 303–356. https://doi.org/10.1006/jhev.2001.0528.

García-González, R., J. M. Carretero, L. Rodríguez, et al. 2009. "Étude analytique d'une clavicule complète de subadulte d'*Homo antecessor* (site de Gran Dolina, Sierra d'Atapuerca, Burgos, Espagne)." *L'Anthropologie* 113, no. 1: 222–232. https://doi.org/10.1016/j.anthro.2008.12.002.

García-Martínez, D., M. Bastir, A. Gómez-Olivencia, et al. 2020. "Early Development of the Neanderthal Ribcage Reveals a Different Body Shape at Birth Compared to Modern Humans." *Science Advances* 6, no. 41: eabb4377. https://doi.org/10.1126/sciadv.abb4377.

García-Martínez, D., O. G. Gil, O. Cambra-Moo, et al. 2017. "External and Internal Ontogenetic Changes in the First Rib." *American Journal of Physical Anthropology* 164, no. 4: 750–762. https://doi.org/10.1002/ajpa.23313.

García-Martínez, D., J. M. López-Rey, O. García Gil, et al. 2023. "How Accurate Are Medical CT and Micro-CT Techniques Compared to Classical Histology When Addressing the Growth of the Internal Rib Parameters?" *Anthropologischer Anzeiger* 80, no. 3: 307–316. https://doi.org/10.1127/anthranz/2023/1617.

García-Martínez, D., N. Torres-Tamayo, I. Torres-Sánchez, F. García-Río, A. Rosas, and M. Bastir. 2018. "Ribcage Measurements Indicate Greater Lung Capacity in Neanderthals and Lower Pleistocene Hominins Compared to Modern Humans." *Communications Biology* 1: 117.

Gómez-Olivencia, A., A. Barash, D. García-Martínez, et al. 2018. "3D Virtual Reconstruction of the Kebara 2 Neandertal Thorax." *Nature Communications* 9: 4387. https://doi.org/10.1038/s41467-018-06803-z.

Gómez-Olivencia, A., J. M. Carretero, C. Lorenzo, J. L. Arsuaga, J. M. Bermúdez de Castro, and E. Carbonell. 2010. "The Costal Skeleton of *Homo antecessor*: Preliminary Results." *Journal of Human Evolution* 59, no. 6: 620–640. https://doi.org/10.1016/j.jhevol.2010.07.023.

Gómez-Olivencia, A., K. L. Eaves-Johnson, R. G. Franciscus, J. M. Carretero, and J. L. Arsuaga. 2009. "Kebara 2: New Insights Regarding the Most Complete Neandertal Thorax." *Journal of Human Evolution* 57, no. 1: 75–90. https://doi.org/10.1016/j.jhevol.2009.02.009.

Gómez-Olivencia, A., T. Holliday, S. Madelaine, C. Couture-Veschambre, and B. Maureille. 2019. "The Costal Skeleton of the Regourdou 1 Neandertal." *Journal of Human Evolution* 130: 151–171. https://doi.org/10.1016/j.jhevol.2017.12.005.

Graeber, G. M., and M. Nazim. 2007. "The Anatomy of the Ribs and the Sternum and Their Relationship to Chest Wall Structure and Function." *Thoracic Surgery Clinics* 17, no. 4: 473–489. https://doi.org/10.1016/j.thorsurg.2006.12.010.

Gray, H. 1878. *Anatomy of the Human Body*. Lea & Febiger.

Haeusler, M., R. Schiess, and T. Boeni. 2011. "New Vertebral and Rib Material Point to Modern Bauplan of the Nariokotome *Homo erectus* Skeleton." *Journal of Human Evolution* 61, no. 5: 575–582. https://doi.org/10.1016/j.jhevol.2011.07.004.

Haile-Selassie, Y., B. M. Latimer, M. Alene, et al. 2010. "An Early *Australopithecus afarensis* Postcranium From Woranso-Mille, Ethiopia." *Proceedings of the National Academy of Sciences* 107: 12121–12126. https://doi.org/10.1073/pnas.1004527107.

Heim, J. L. 1976. *Les Hommes fossiles de la Ferrassie. I. Le gisement. Les squelettes adultes (crâne et squelette du tronc)*. Masson.

Holcombe, S. A., and B. A. Derstine. 2022. "Rib Cortical Bone Thickness Variation in Adults by Age and Sex." *Journal of Anatomy* 241, no. 6: 1344–1356. https://doi.org/10.1111/joa.13751.

Jellema, L. M., B. Latimer, and A. Walker. 1993. "The Rib Cage." In *The Nariokotome Homo Erectus Skeleton*, edited by A. Walker and R. Leakey, 294–325. Harvard University Press.

Kors, C., A. González-Ruiz, M. J. Goncalves, M. J. Valente, C. Garcia, and H. F. Cardoso. 2025. "The Impact of Social, Economic and Political Change in Linear and Appositional Growth of Children From the Medieval Islamic and Christian Periods of the Algarve, Portugal." *Journal of Archaeological Science* 62: 105018. https://doi.org/10.1016/j.jasrep.2025.105018.

Lewis, M., F. Shapland, and R. Watts. 2016. "On the Threshold of Adulthood: A New Approach for the Use of Maturation Indicators to Assess Puberty in Adolescents From Medieval England." *American Journal of Human Biology* 28, no. 1: 48–56. https://doi.org/10.1002/ajhb.22761.

Liversidge, H. M., and P. H. Marsden. 2010. "Estimating Age and the Likelihood of Having Attained 18 Years of Age Using Mandibular Third Molars." *British Dental Journal* 209, no. 8: E13. https://doi.org/10.1038/sj.bdj.2010.976.

López-Rey, J. M., O. Cambra-Moo, A. González Martín, et al. 2022. "Mineral Content Analysis in the Rib Cross-Sections of *Homo sapiens* and *Pan troglodytes* and Its Implications for the Study of Sts 14 Costal Remains." *American Journal of Biological Anthropology* 177, no. 4: 784–791. https://doi.org/10.1002/ajpa.24491.

López-Rey, J. M., Ó. Cambra-Moo, A. González Martín, et al. 2023. "Covariation Between the Shape and Mineralized Tissues of the Rib Cross Section in *Homo sapiens*, *Pan troglodytes* and Sts 14." *American Journal of Biological Anthropology* 183, no. 1: 157–164. https://doi.org/10.1002/ajpa.24844.

López-Rey, J. M., I. Crevecoeur, H. May, et al. 2025. "Ancient Ribcages, Modern Form: New Insights Into *Homo sapiens* Evolution." *Communications Biology* 8: 1038. https://doi.org/10.1038/s42003-025-08472-3.

López-Rey, J. M., D. M. Doe, O. Cambra-Moo, A. González Martín, and D. García-Martínez. 2025. "Mineralized Area of the Human Rib

26927691, 2026, 2, Downloaded from https://onlinelibrary.wiley.com/doi/10.1002/ajpa.70299 by Universidad De Burgos, Wiley Online Library on [31/07/2026]. See the Terms and Conditions (https://onlinelibrary.wiley.com/terms-and-conditions) on Wiley Online Library for rules of use; OA articles are governed by the applicable Creative Commons License

Cross-Sections From Early Puberty Until Adulthood." *Anatomical Record (Hoboken, N.J. : 2007)* 309: 649–656. https://doi.org/10.1002/ar.70001.

López-Rey, J. M., D. García-Martínez, and M. Bastir. 2025. "Shanidar 3 'Rings the Bell': Virtual Ribcage Reconstruction and Its Implications for Understanding the Neanderthal Bauplan." *Journal of Human Evolution* 199: 103629. https://doi.org/10.1016/j.jhevol.2024.103629.

Manifold, B. M. 2012. "Intrinsic and Extrinsic Factors Involved in the Preservation of Non-Adult Skeletal Remains in Archaeology and Forensic Science." *Bulletin of The International Association For Paleodontology* 6: 51–69.

Moorrees, C. F. A., E. A. Fanning, and E. E. Hunt. 1963. "Age Variation of Formation Stages for Ten Permanent Teeth." *Journal of Dental Research* 42, no. 6: 1490–1502. https://doi.org/10.1177/00220345630420062701.

Murail, P., J. Bruzek, F. Houët, and E. Cunha. 2005. "DSP: A Tool for Probabilistic Sex Diagnosis Using Worldwide Variability in Hip-Bone Measurements." *Bulletins et Mémoires de la Société d'Anthropologie de Paris* 17: 167–176. https://doi.org/10.4000/bmsap.1157.

Phenice, T. W. 1969. "A Newly Developed Visual Method of Sexing the Os Pubis." *American Journal of Physical Anthropology* 30, no. 2: 297–301. https://doi.org/10.1002/ajpa.1330300214.

R Core Team. 2023. *R: A Language and Environment for Statistical Computing*. R Foundation for Statistical Computing. https://www.r-project.org/.

Rascón Pérez, J., M. Campo Martín, Ó. Cambra-Moo, G. Pimentel de Francisco, and A. G. González Martín. 2013. "Distribución diferencial de caracteres de interés patológicos y no patológicos por edad y sexo en el cementerio medieval de Veranes (Gijón)." In *Vetera corpora morbo afflicta: Actas del XI Congreso Nacional de Paleopatología*, edited by A. Malgosa, A. Isidro, P. Ibáñez-Gimeno, and G. Prats-Muñoz, 607–634. Universidad Autónoma de Barcelona.

Ríos, L., and H. F. Cardoso. 2009. "Age Estimation From Stages of Union of the Vertebral Epiphyses of the Ribs." *American Journal of Physical Anthropology* 140, no. 2: 265–274. https://doi.org/10.1002/ajpa.21065.

Ryan, T. M., and C. N. Shaw. 2015. "Gracility of the Modern *Homo sapiens* Skeleton Is the Result of Decreased Biomechanical Loading." *Proceedings of the National Academy of Sciences* 112, no. 2: 372–377. https://doi.org/10.1073/pnas.1418646112.

Schindelin, J., I. Arganda-Carreras, E. Frise, et al. 2012. "Fiji: An Open-Source Platform for Biological-Image Analysis." *Nature Methods* 9, no. 7: 676–682. https://doi.org/10.1038/nmeth.2019.

Schmid, P. 1983. "A Reconstruction of the Skeleton of a.L. 288-1 (Hadar) and Its Consequences." *Folia Primatologica* 40, no. 4: 283–306. https://doi.org/10.1159/000156111.

Schmid, P., S. E. Churchill, S. Nalla, et al. 2013. "Mosaic Morphology in the Thorax of *Australopithecus sediba*." *Science* 340, no. 6129: 1234598. https://doi.org/10.1126/science.1234598.

Schotsmans, E. M., N. Márquez-Grant, and S. L. Forbes, eds. 2017. *Taphonomy of Human Remains: Forensic Analysis of the Dead and the Depositional Environment*. John Wiley & Sons.

Shapland, F., and M. E. Lewis. 2013. "Brief Communication: A Proposed Osteological Method for the Estimation of Pubertal Stage in Human Skeletal Remains." *American Journal of Physical Anthropology* 151, no. 2: 302–310. https://doi.org/10.1002/ajpa.22268.

Shapland, F., and M. E. Lewis. 2014. "Brief Communication: A Proposed Method for the Assessment of Pubertal Stage in Human Skeletal Remains Using Cervical Vertebrae Maturation." *American Journal of Physical Anthropology* 153, no. 1: 144–153. https://doi.org/10.1002/ajpa.22416.

Smith, S. L. 2004. "Skeletal Age, Dental Age, and the Maturation of KNM-WT 15000." *American Journal of Physical Anthropology* 125, no. 2: 105–120. https://doi.org/10.1002/ajpa.10376.

Trinkaus, E. 1983. *The Shanidar Neandertals*. Academic Press.

Turner–Walker, G., and U. Syversen. 2002. "Quantifying Histological Changes in Archaeological Bones Using BSE–SEM Image Analysis." *Archaeometry* 44, no. 3: 461–468. https://doi.org/10.1111/1475-4754.t01-1-00078.

Vandermeersch, B. 1981. *Les hommes fossiles de Qafzeh (Israël)*. Éditions du CNRS.

Walker, A. 1993. "Chapter 4: Taphonomy." In *The Nariokotome Homo erectus Skeleton*, edited by A. Walker and R. E. Leakey, 40–53. Harvard University Press.

Wickham, H. 2016. *ggplot2: Elegant Graphics for Data Analysis*. Springer-Verlag.

Wickham, H., R. François, L. Henry, K. Müller, and D. Vaughan. 2023. "dplyr: A Grammar of Data Manipulation." R package version 1.1.4. https://github.com/tidyverse/dplyr.

Wickham, H., D. Vaughan, and M. Girlich. 2024. "tidyr: Tidy Messy Data." R package version 1.3.1. https://github.com/tidyverse/tidyr.

Wilson, L. A., and L. T. Humphrey. 2015. "A Virtual Geometric Morphometric Approach to the Quantification of Long Bone Bilateral Asymmetry and Cross-Sectional Shape." *American Journal of Physical Anthropology* 158, no. 4: 541–556. https://doi.org/10.1002/ajpa.22809.

Supporting Information

Additional supporting information can be found online in the Supporting Information section. **Table S1:** Rib cross-sectional relative bone area (%) of the full *H. sapiens* sample.

26927691, 2026, 2, Downloaded from https://onlinelibrary.wiley.com/doi/10.1002/ajpa.70299 by Universidad De Burgos, Wiley Online Library on [31/07/2026]. See the Terms and Conditions (https://onlinelibrary.wiley.com/terms-and-conditions) on Wiley Online Library for rules of use; OA articles are governed by the applicable Creative Commons License